Coupling of a Planar Waveguide and a Dielectric Disk

Rohinton S. Dehmubed, *Member, IEEE,* and Paul Diament

***Abstract*—The complete analytic solution to the problem of coupling between a slab waveguide and a ring has been derived. The two-configuration problem is reduced to two simultaneous single-configuration problems by the method of equivalence. These are independently solved to yield the exact solution in terms of modal content. The results are illustrated with a numerical example and corroborated independently by a variational approach.**

***Index Terms*—Coupling, ring lasers, ring resonators.**

I. Introduction

RING LASERS [1]–[3] show great potential as light sources for monolithic integration. The resonator is a ring, rather than a pair of mirrors. A waveguide in close proximity to the ring provides the output coupling. The resonator requires no cleaving and the ring can be defined photolithographically, which means better control over the cavity length and topology of the design. The alternative distributed feedback (DFB) and distributed Bragg reflector (DBR) lasers need gratings of some sort, which make their fabrication a relatively complex task. Ring lasers, by comparison, are much simpler to fabricate, especially the index-guided rib waveguide structures.

Quite a few papers characterizing the ring laser and its fabrication technology have been published, revealing substantial improvement in fabrication and materials technology. The most recent publications show that high-power single-frequency ring lasers, along with detectors, can be made on a substrate without resorting to cleaving [4]–[7].

The analysis of lasers begins with that of the resonator. Indeed, a better understanding of the basic mechanisms of mode coupling and excitation efficiency can help in designing these as yet not fully understood devices. The semiconductor ring laser's operating characteristics depend strongly on the back reflections and coupling between the counter-propagating modes [8], [9]. The output waveguide coupler also affects the performance [10].

The general methods of analyzing such ring lasers treat the waveguide coupler and ring as separate discrete optical elements. This approximation provides an accurate model only if the ring and coupler lengths are much larger than the wavelength. This approach provides no information about the backscattered radiation, which may be highly pertinent to the design. The curved region is usually modeled as a waveguide with losses due to radiation from the curved surfaces. This can be analyzed by a variety of methods, including the Wentzel, Krammers, Brillouin (WKB) approximation, conformal mapping [11], and the wide-angle beam propagation method (BPM). These methods are appropriate as long as the radius of curvature is much greater than the wavelength. The analysis breaks down completely in the region where the radius of curvature is of the order of the wavelength.

The other numerical methods that can be used to solve the problem are the FEM (finite-element method) and BEM (boundary-element method) [12]. Both of these are relatively complex, and do not give a good intuitive understanding of the problem. The FEM also suffers from spurious solutions. The BPM, even when applicable, does not give the backscattered radiation.

We have developed a method to solve this problem in its entirety. The scattered field is given as a distribution of the modes of the waveguide. The analytic solution obtained is applicable for all values of the parameters and gives considerable insight into the problem. The approach is to reduce the complex configuration to two separate simple ones based on the equivalence principle.

This paper is organized as follows. Section II defines the problem and reduces it to two simpler problems. In Sections III and IV, we solve these reduced problems. Finally, in Section V, the results are put together to obtain the solution.

II. Problem Definition

Fig. 1 shows a dielectric slab waveguide in proximity to, and exciting, a dielectric slab ring. The n's are the refractive indexes at the frequency of excitation. S is the input optical source exciting the waveguide; this could be a butt-coupled fiber, laser diode, or focused beam of light. The arrow indicates the direction of propagation of the input wave. The unknown $\boldsymbol{F}$ represents the field distribution for the structure; it is the complete vector field (electric and magnetic) excited by this source.

In the following sections, the equivalence principle of electromagnetic theory [13, pp. 37–39] and the superposition principle for electromagnetic waves are used to reduce the problem to simpler equivalents [13, Ch. 1 and 2].

A. Conversion of Two-Configuration Problem into Two Single-Configuration Problems

Consider the dielectric slab waveguide alone, as shown in Fig. 1(b)—the ring is absent. Let $\boldsymbol{F_i}$ be the field excited in this configuration by the input source S of the original problem.

Manuscript received May 28, 1997; revised March 9, 1998.

R. S. Dehmubed is with TranSwitch Corporation, Shelton, CT 06484 USA.

P. Diament is with the Department of Electrical Engineering, Columbia University, New York, NY 10027 USA.

Publisher Item Identifier S 0018-9480(98)07241-X.

0018–9480/98$10.00 © 1998 IEEE

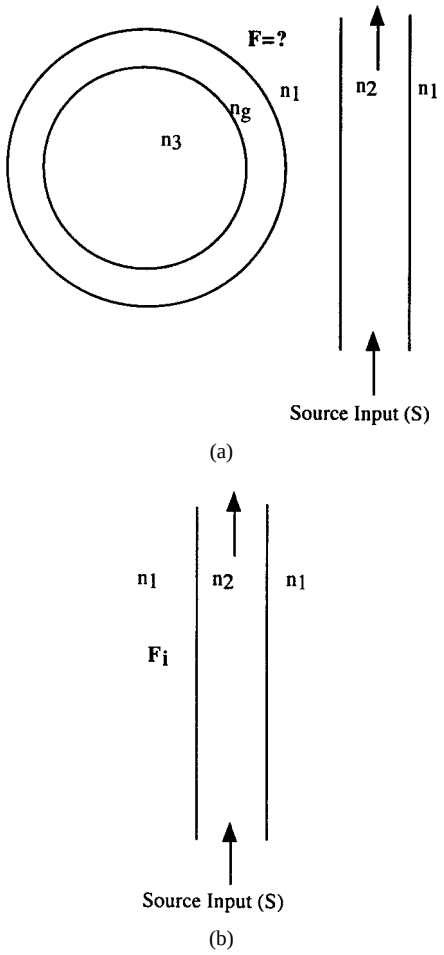

Fig. 1. The original problem's waveguide and ring.

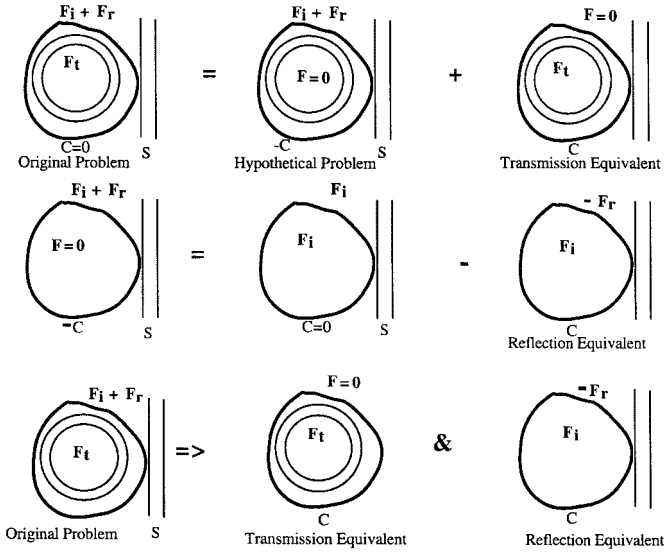

Fig. 2. The conversion of a two-configuration problem into two equivalent single-configuration problems.

This is the complete field, including both the electric and magnetic parts. This field is considered known; in fact, we specify the source S by giving its resultant field $\boldsymbol{F_i}$. The solution to the original problem, the field $\boldsymbol{F}$, is expressed as a superposition of the incident field $\boldsymbol{F_i}$ and a "scattered" field. To reduce the one complicated problem to two simple ones, we partition the space into two regions, defined by the interior and exterior of an imaginary surface we call the separatrix. The scattered field is comprised of a "reflected" field $\boldsymbol{F_r}$ outside the arbitrary surface (curve in cross section) and a "transmitted" field $\boldsymbol{F_t}$ inside the surface. The separatrix is shown in cross section (in bold) in the first diagram of Fig. 2.

Consider a hypothetical problem in which the field inside the separatrix is forced to be zero, while the field outside the separatrix is maintained exactly as in the original problem (see the second diagram of Fig. 2). In order to have zero field inside the hypothetical closed region, but not outside, there must exist surface current sources on the separatrix. The surface in this case is cylindrical with its axis normal to the plane of the paper. The current source is labeled $\boldsymbol{C}$ in the figure; as per Maxwell's equations, it is equal in strength and perpendicular to the discontinuity in the tangential field and imposes the assumed discontinuity in the field. It is, in general, composed of both electric and magnetic currents. Mathematically defined magnetic currents are needed here to impose the purely hypothetical discontinuity in tangential electric field, from the incident plus scattered field outside the region to zero inside [13].

Using superposition, the original problem is reduced to two configurations: the "hypothetical" one and a "transmission equivalent," as shown in the first row of Fig. 2. The transmission equivalent will be simplified, but consider first the hypothetical problem. There are two sources in this modified configuration: one is the input source S, the other is the electric and magnetic surface current $\boldsymbol{C}$ on the separatrix. This configuration may be decomposed into a superposition of two partial problems, each with only one of the sources, as in the second row of Fig. 2.

Since the field inside the separatrix is zero, the interior region's index (permittivity) may be altered to any other one, as this cannot affect the zero field. The arbitrary index distribution chosen is the uniform distribution with the index of the region immediately outside the separatrix. The hypothetical problem is now reduced to a "reflection equivalent," in which the field inside the separatrix is the "incident field" $\boldsymbol{F_i}$ that defines the source, while the field outside, $-\boldsymbol{F_r}$, is the negative of the "reflected field" of the original problem.

In the transmission equivalent, the external waveguide can be dropped, as this can not affect the zero field. The current $\boldsymbol{C}$ is equal to the discontinuity in the field, viz., $\boldsymbol{F_t}$ at the separatrix. The last row of the figure shows that the scattered fields of the original waveguide-and-ring problem can be obtained from two equivalent versions, one with only the ring and the other with only the waveguide.

B. Equivalent Problem

The final result so obtained from Fig. 2 is depicted in Fig. 3. The original problem has been broken down into the superposition of the input field $\boldsymbol{F_i}$ and a scattered field obtainable from two "single-configuration" problems. These are the *transmission* and *reflection equivalents*. The shape of the separatrix has been chosen as a circular cylinder.

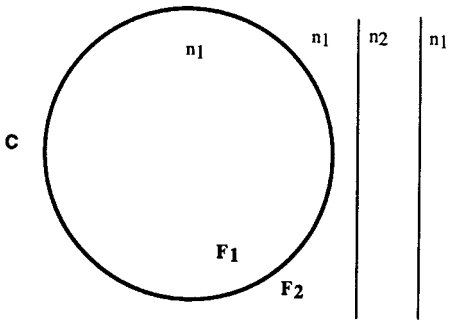

(a)

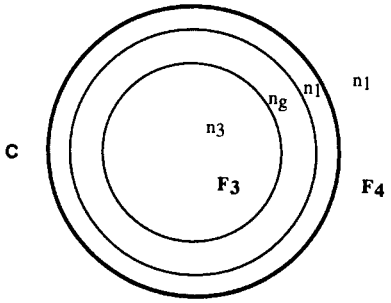

(b)

Fig. 3. The equivalent two single-configuration problems. (a) Reflection equivalent. (b) Transmission equivalent.

At first glance, things may not look any simpler, in that the surface current $\boldsymbol{C}$ is expressed in terms of discontinuities in $\boldsymbol{F_t}$, an unknown. The way to make use of this decomposition is to solve each of the two single-configuration problems independently, for any arbitrary specified current-source $\boldsymbol{C}$. Then use is made of the fact that this current source is the same for both the problems.

In short—from the Green's function for each of the two single-configuration problems, find the fields for any (arbitrary, but specified) current-source $\boldsymbol{C}$. From this, determine the current that generates both

$$\boldsymbol{F_1 = F_i}$$

and

$$\boldsymbol{F_4 = 0.}$$

These two conditions should allow solution for the current $\boldsymbol{C}$. Once the current $\boldsymbol{C}$ has been found, use the same Green's functions to determine the fields

$$\boldsymbol{F_2 = -F_r}$$

and

$$\boldsymbol{F_3 = F_t.}$$

Except for the sign of $\boldsymbol{F_2}$, these are the exact fields that were sought, without approximation.

III. The Transmission Equivalent

In Section II, it was shown that the ring resonator problem can be reduced to two independent, but simultaneous, problems: the *transmission* and the *reflection equivalents*. In this section, the problem defined as the *transmission equivalent* is addressed, as described in Fig. 4. R is the radius of the circular separatrix that carries the surface current $\boldsymbol{C}$. n_1, n_g, and n_3 are the indexes of refraction of the various regions of the optical ring and r_1, r_2 are its inner and outer radii.

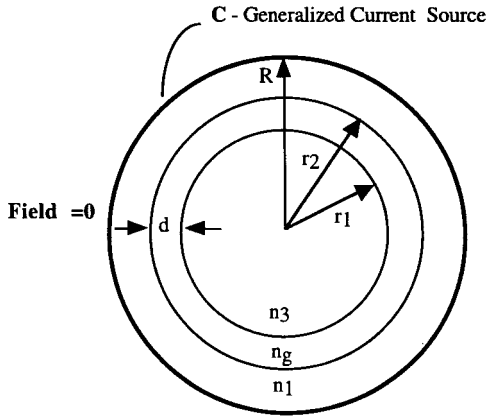

Fig. 4. Transmission equivalent.

In the transmission equivalent, we need to solve for $\boldsymbol{C}$ subject to the condition that the field outside the ring is zero. Since the current $\boldsymbol{C}$ is, in general, composed of both electric and magnetic components, this results in a relation between the two currents. For the geometry of the transmission equivalent, the general field can be split into separate TE and TM modes [14, Ch. 8, p. 306]. In the simpler case of TE waves, the field is given by the three components $\{\mathcal{E}_y(r,\theta), \mathcal{H}_\theta(r,\theta), \mathcal{H}_r(r,\theta)\}$. The y-axis is normal to the plane of the paper.

A. Fields and Their Description

Due to the circular symmetry, the electric field must be of the form

$$\mathcal{E}_y(r,\theta) = \sum_{l=-\infty}^{\infty} \{A_l J_l(k_0 n_1 r) + B_l Y_l(k_0 n_1 r)\} e^{jl\theta}, \quad r_2 \le r < R \quad (1)$$

$$\mathcal{E}_y(r,\theta) = \sum_{l=-\infty}^{\infty} \{C_l J_l(k_0 n_g r) + D_l Y_l(k_0 n_g r)\} e^{jl\theta}, \quad r_1 \le r < r_2 \quad (2)$$

$$\mathcal{E}_y(r,\theta) = \sum_{l=-\infty}^{\infty} E_l J_l(k_0 n_3 r) e^{jl\theta}, \qquad 0 \le r < r_1 \quad (3)$$

$$\mathcal{E}_y(r,\theta) = 0, \qquad r > R \quad (4)$$

k_0 is the free-space propagation constant. J_l and Y_l are the Bessel functions of order l of the first and second kind, respectively.

The boundary conditions of continuity of tangential electric and magnetic fields is applied at each interface, except for the prescribed discontinuity at $r = R$, due to $\boldsymbol{C}$. A two-dimensional (2-D) case has been assumed by ignoring variation along the y-axis. The boundary condition translates into continuity of $\mathcal{E}^y(r,\theta)$ and $(\partial/\partial r)\mathcal{E}_y(r,\theta)$ across the boundaries. The circle of field discontinuity carries electric current along y and magnetic current along θ.

B. Current-Source Description

The unknown current-source $\boldsymbol{C}$ consists of two independent surface currents: electric current-source $\mathcal{J}_e$ and magnetic current-source $\mathcal{J}_m$. Expand these current sources as Fourier series as follows:

$$\mathcal{J}_e = \sum_{l=-\infty}^{\infty} e_l \, e^{jl\theta} \tag{5}$$

$$\mathcal{J}_m = \sum_{l=-\infty}^{\infty} m_l \, e^{jl\theta} \tag{6}$$

where e_i, m_i are the ith electric and magnetic currents' Fourier series components, respectively.

The complete solution can be obtained once the current $\boldsymbol{C}$ (composed of $\mathcal{J}_e$ and $\mathcal{J}_m$) is found by solving the transmission and reflection equivalents simultaneously. The transmission equivalent gives the relation governing $\mathcal{J}_e$ and $\mathcal{J}_m$ in order to have the field outside the current ring $(r > R)$ equal zero.

The result is that (see Appendix), for the field outside the circle to be zero, the following condition has to be satisfied:

$$e_l = j \, \frac{k_0 n_1}{\omega \mu_0} \, b_l \, C_l'(k_0 n_1 R) \, \hat{y} \tag{7}$$

$$m_l = -b_l \, C_l(k_0 n_1 R) \, \hat{\theta} \tag{8}$$

where b_l is a constant:

1) $C_l(k_0 n_1 R) = J_l(k_0 n_1 R) + \Delta_l \, Y_l(k_0 n_1 R)$ is a cylinder function;
2) $\Delta_l = B_l / A_l$ is given by (61);
3) k_0 is the free-space propagation constant;
4) n_1 is the refractive index of the cladding;
5) R is the radius of the current-carrying circle;
6) J_l, Y_l are the Bessel functions of order l.

Also note that, in all the above expressions, n_1, n_g, n_3 are arbitrary indexes, i.e., n_g can be less than n_1, n_3, or any other combination thereof.

IV. Reflection Equivalent

This problem is slightly more complex than the transmission equivalent. We begin by stating one of the many forms of the Lorentz reciprocity theorem (LRT). This will be used to solve the problem of waveguide excitation by the surface currents. The results of this section will be used later to find the normal modes of the waveguide excited by the current source. Finally, we apply the forcing condition of the reflection equivalent, namely, that the field inside the current ring should equal the input excitation $\boldsymbol{F_i}$.

A. LRT

The LRT applied to the waveguide-excitation problem [13, Ch. 7] is

$$\iint_S (\mathcal{E} \times H_n - E_n \times \mathcal{H}) \cdot dS = \iiint_V (\mathcal{J}_e \cdot E_n - \mathcal{J}_m \cdot H_n) \, dV \tag{9}$$

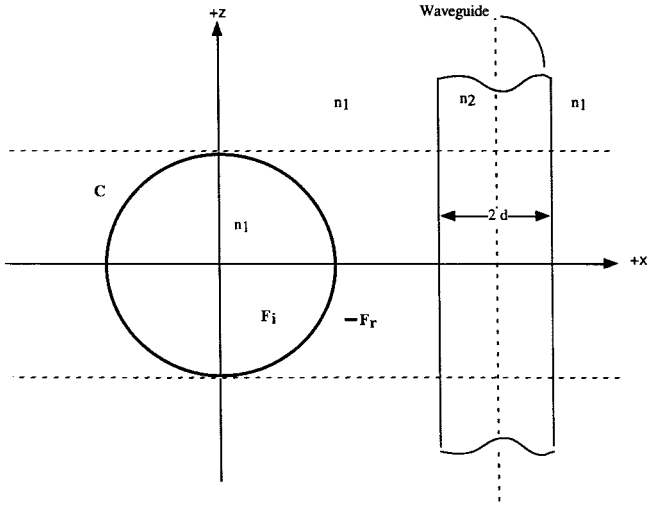

Fig. 5. Reflection equivalent, waveguide excitation by a current-source C.

where V is an arbitrary volume enclosing the current-sources $\mathcal{J}_e$, $\mathcal{J}_m$ and S is the surface bounding the volume. dV and dS are the volume and surface element vectors (directed outward), respectively. $\mathcal{J}_e$, $\mathcal{J}_m$ are the electric and magnetic (volume) current sources of the fields $\mathcal{E}$, $\mathcal{H}$, while E_n, H_n are the sourceless normal modes.

Consider a current-source $\boldsymbol{C}$ near a dielectric waveguide, as shown in Fig. 5. Let $\mathcal{E}(x,z)$ and $\mathcal{H}(x,z)$ be the fields generated by this source. The problem is reduced to two dimensions (in x and z) by ignoring the variation along the y-axis. Let the set $\{E_n(x,z), H_n(x,z)\}$ be the modes of the waveguide satisfying the homogeneous wave equation, i.e., the source-free solutions. These modes are solutions of the Helmholtz equation and form a complete orthogonal set. They consist of a finite number of guided modes and a continuum of radiation modes. Since the modes form a complete set, the field $\mathcal{W}(x,z)$ can be expressed as

$$\mathcal{W}(x,z) = \sum_n a_n^+(z) W_n^+(x,z) + \sum_n a_n^-(z) W_n^-(x,z). \tag{10}$$

The superscripts $+$ and $-$ signify forward-propagating and backward-propagating waves, respectively. $\mathcal{W}(x,z) = [\mathcal{E}(x,z), \mathcal{H}(x,z)]$, $W_n(x,z) = [E_n(x,z), H_n(x,z)]$, $E_n(x,z)$, and $H_n(x,z)$ are vector fields described by [13, Ch. 7]

$$E_n^+(x,z) = [e_n(x) + e_{zn}(x)] e^{-j\beta_n z} \tag{11}$$

$$E_n^-(x,z) = [e_n(x) - e_{zn}(x)] e^{+j\beta_n z} \tag{12}$$

$$H_n^+(x,z) = [h_n(x) + h_{zn}(x)] e^{-j\beta_n z} \tag{13}$$

$$H_n^-(x,z) = [-h_n(x) + h_{zn}(x)] e^{+j\beta_n z} \tag{14}$$

where the subscript zn signifies the axial component of the nth mode's vector field. For convenience, we retain the summation sign for the continuum; however, strictly speaking, it should be replaced by summation over the guided modes and integration over the continuum. The normalization condition is written as

$$\int_{-\infty}^{+\infty} e_n \times h_m \cdot dA_z = \delta_{nm}.$$

Thus, E_n and H_n form a complete orthonormal set.

Here, we had to incorporate the backward-propagating modes into the most general solution, denoted by the negative superscript. In order to have a consistent sign for the Poynting vector, the coefficient $h_n(x)$ must have a negative sign in the magnetic field $H_n^-(x,z)$ [16, pp. 14, 15] [14, Ch. 8, p. 323].

Expanding $\mathcal{E}$ and $\mathcal{H}$ in terms of their normal modes, substituting for E_n and H_n, and noting the normalization results in

$$a_n^-(z_1) - a_n^-(z_2) = +\tfrac{1}{2} \iiint_V (\mathcal{J}_e \cdot E_n^+ - \mathcal{J}_m \cdot H_n^+)\, dV \tag{15}$$

$$a_n^+(z_2) - a_n^+(z_1) = -\tfrac{1}{2} \iiint_V (\mathcal{J}_e \cdot E_n^- - \mathcal{J}_m \cdot H_n^-)\, dV \tag{16}$$

where $-R \le z_1 \le z_2 \le +R$ and V is the volume enclosed by the planes $z = z_1$ and $z = z_2$.

For the surface current $\boldsymbol{C}$, the volume integral reduces to a one-dimensional integral around the contour of the circle within the volume V (see Fig. 5). Now, the physical constraints that the currents can only radiate outward are applied as follows:

$$a_n^+(-R) = 0$$

and

$$a_n^-(+R) = 0.$$

This results in the following expression for $a_n(z)$ for $-R \le z \le +R$:

$$a_n^+(z) = -\tfrac{1}{2} \int_{C_1(z)} (\mathcal{J}_e \cdot E_n^- - \mathcal{J}_m \cdot H_n^-)\, dl \tag{17}$$

$$a_n^-(z) = -\tfrac{1}{2} \int_{C_2(z)} (\mathcal{J}_e \cdot E_n^+ - \mathcal{J}_m \cdot H_n^+)\, dl \tag{18}$$

and

$$a_n^+(+R) = -\tfrac{1}{2} \oint_C (\mathcal{J}_e \cdot E_n^- - \mathcal{J}_m \cdot H_n^-)\, dl \tag{19}$$

$$a_n^-(-R) = -\tfrac{1}{2} \oint_C (\mathcal{J}_e \cdot E_n^+ - \mathcal{J}_m \cdot H_n^+)\, dl \tag{20}$$

where $C_1(Z)$ is the fraction of circle (contour) enclosed by the planes $z = -R$ and $z = Z$, $C_2(Z)$ is the fraction of circle (contour) enclosed by the planes $z = +R$ and $z = Z$ (see Fig. 6). The contour C is the complete current loop, which is the contour defined by $C_1(+R)$ or $C_2(-R)$. The a's are the components of the scattered electric field [13, pp. 359–361]. These equations are valid for the continuum modes as well.

B. Condition Imposed on the Field

Equations (17) and (18) describe the normal field excitations $a_n(z)$ in terms of the overlap integral of the normal modes and currents. These are contour integrals around a circular sector. The currents $\mathcal{J}_e$ and $\mathcal{J}_m$ are expressed in terms of their Fourier series. This integral has to be evaluated for an arbitrary circular arc in order to express the field excited by the current ring in the region $-R \le z \le +R$. A convenient way to evaluate this integral is by Fourier-series decomposition of the normal fields E_n and H_n. The obvious choice is the cylindrical coordinate system (r, θ, y) at the current ring center. The contour integral is then reduced to a sum of complex exponentials.

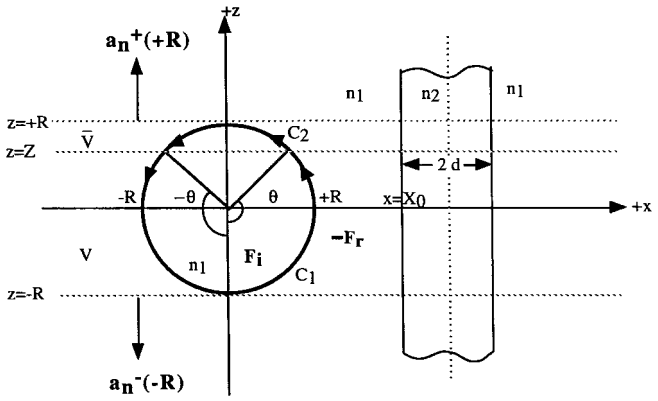

Fig. 6. Contour of integration.

1) Evaluation of $a(z)$: The modes can be separated into TE and TM, and are each independently considered. Consider the TE field (see Fig. 6). Expanding the normal modes as a Fourier series,

$$E_n^+(x,z) = \sum_k J_k(k_0 n_1 r)\mathcal{A}_k(+n) e^{jk\theta}\, \hat{y} \tag{21}$$

$$H_n^+(x,z) = \sum_k -j\, \frac{k_0 n_1}{\omega\mu_0}\, J_k'(k_0 n_1 r)\mathcal{A}_k(+n) e^{jk\theta}\, \hat{\theta} \tag{22}$$

$$E_n^-(x,z) = \sum_k J_k(k_0 n_1 r)\mathcal{A}_k(-n) e^{jk\theta}\, \hat{y} \tag{23}$$

$$H_n^-(x,z) = \sum_k -j\, \frac{k_0 n_1}{\omega\mu_0}\, J_k'(k_0 n_1 r)\mathcal{A}_k(-n) e^{jk\theta}\, \hat{\theta}. \tag{24}$$

Let e_l and m_l be the Fourier components of the electric and magnetic current source, respectively. For convenience, define

$$m_l' = -j\, \frac{k_0 n_1}{\omega\mu_0} m_l. \tag{25}$$

From (17), (18), and the above expressions for the normal modes (21)–(24),

$$a_n^+(z) = -\tfrac{1}{2} \sum_l \sum_k [e_l\, J_k(k_0 n_1 R) - m_l'\, J_k'(k_0 n_1 R)] \cdot \mathcal{A}_k(-n) \int_{C_1(\theta)} e^{j(k+l)\theta'} R\, d\theta' \tag{26}$$

similarly,

$$a_n^-(z) = -\tfrac{1}{2} \sum_l \sum_k [e_l\, J_k(k_0 n_1 R) - m_l'\, J_k'(k_0 n_1 R)] \cdot \mathcal{A}_k(+n) \int_{C_2(\theta)} e^{j(k+l)\theta'} R\, d\theta' \tag{27}$$

where $z = -R\cos\theta$ for $0 \le \theta \le +\pi$ and

$$a_n^-(-R) = -\pi R \sum_l [e_{-l}\, J_l(k_0 n_1 R) - m_{-l}'\, J_l'(k_0 n_1 R)]\mathcal{A}_l(+n) \tag{28}$$

$$a_n^+(+R) = -\pi R \sum_l [e_{-l}\, J_l(k_0 n_1 R) - m'_{-l}\, J'_l(k_0 n_1 R)]\mathcal{A}_l(-n). \quad (29)$$

C. Evaluation of the Radiated Field in Terms of Normal Modes

The required integrals are

$$R \int_{C_1\,(\theta)} e^{jm\theta'}\, d\theta' = f_m^+(\theta) = 2R\theta, \qquad m = 0 \quad (30)$$

$$f_m^+(\theta) = 2R\,\frac{\sin m\theta}{m}, \qquad m \neq 0 \quad (31)$$

and

$$R \int_{C_2(\theta)} e^{jm\theta'}\, d\theta' = f_m^-(\theta) = 2R\,(\pi - \theta), \qquad m = 0 \quad (32)$$

$$f_m^-(\theta) = -f_m^+(\theta) = -2R\,\frac{\sin m\theta}{m}, \qquad m \neq 0. \quad (33)$$

Note that $0 \leq \theta \leq \pi$ and $z = -R\cos\theta$.

Substituting for $a_n(z)$ and the Fourier series for the normal modes, and rewriting the resultant field as a Fourier series, (10), (17), and (18) result in

$$\mathcal{W}(x,z) = -\frac{1}{2} \sum_{l,k,n} (e_l J_k - m'_l J'_k) \cdot \left\{ \mathcal{A}_k(-n)\, f_{l+k}^+\left(\cos^{-1}\left[\frac{-z}{R}\right]\right) W_n^+(x,z) + \mathcal{A}_k(+n)\, f_{l+k}^-\left(\cos^{-1}\left[\frac{-z}{R}\right]\right) W_n^-(x,z) \right\} \quad (34)$$

where W_n is the complete field vector $[E_n, H_n]$. The argument of J_k is dropped for convenience, but is understood to be $k_0 n_1 R$. Equation (34) gives the field $\mathcal{W}(x,z)$ for all $-R < z < +R$.

D. Forcing Condition

We now apply the condition of the reflection equivalent. For reflection equivalence, the field in the region interior to the current ring (the separatrix), i.e., $0 < r < R$, is forced to equal $\mathcal{F}_i$, the input excitation. Substituting for the currents e_l and m_l from the transmission equivalent (7), (8),

$$\mathcal{F}_i(x,z) = \frac{jn_1 k_0}{2\omega\mu_0} \sum_{l,k,n} b_l (C'_l J_k - C_l J'_k) \cdot [\mathcal{A}_k(-n)\, f_{l+k}^+(\theta)\, W_n^+(x,z) + \mathcal{A}_k(+n)\, f_{l+k}^-(\theta)\, W_n^-(x,z)] \quad (35)$$

for $0 < \sqrt{x^2+z^2} < R$, with $\theta = cos^{-1}(-z/R)$. This equation is to yield the unknown coefficients b_l.

V. Numerical Results

The technique is finally illustrated with an example. The above results are easily extended to TM modes as well. Their analysis is analogous to that of the TE modes and are not reported explicitly.

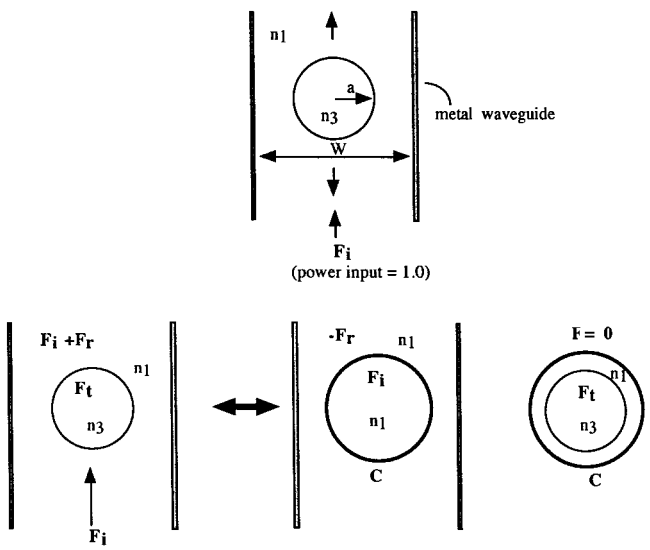

Fig. 7. Scattering by a dielectric disk inside a metal-clad waveguide. The problem has been shown in terms of its reflection and transmission equivalents.

A. Scattering by a Dielectric Disk Inside a Metal-Clad Slab Waveguide

Fig. 7 shows the problem of a simple dielectric disc inside a metal-clad waveguide. The waveguide walls are assumed lossless. The width W of the waveguide is chosen such that it is a single-mode waveguide. That is to say, it supports only one TE mode: the TE_1 mode. The problem is shown in terms of its reflection and transmission equivalents. n_1 and n_3 are the refractive indexes of the material filling the waveguide and the disk, respectively.

1) Data-Fitting Approach: From (35), we can see that the problem is reduced to finding an optimal set of $b_l C_l$ that minimizes the error in $\mathcal{E}(x,z)$. This is essentially a 2-D (i.e., in x and z) data-fitting problem. This method of solution is highly generalized and is applicable to both continuum (dielectric waveguides) and discrete mode problems.

Setting up such problems requires elaborate numerical programming and memory management, which is nothing new, and has been done routinely. For this paper, it was carried out for a small number of terms to illustrate the principle. This can be easily scaled up for a more elaborate problem (see Fig. 8).

Depending on how the summations over the modes (integrations in case of a continuum) are to be performed, either $\mathcal{E}(r,\theta)$ or $\mathcal{E}(x,z)$ can be used for the point matching. Once the vector $b_l C_l$ is obtained, it is a simple inner-product operation to obtain the scattered modes. They are given as

$$a_\beta^-(-R) = -\frac{2j}{\omega\mu_0} \sum_k b_k \Delta_k (-1)^k \mathcal{A}_{-k}^+(\beta) \quad (36)$$

$$a_\beta^+(+R) = -\frac{2j}{\omega\mu_0} \sum_k b_k \Delta_k (-1)^k \mathcal{A}_{-k}^-(\beta). \quad (37)$$

As a final note, the expression for the scattered field is exact in terms of the currents. One is not limited to point-matching to obtain the vector $b_l C_l$, but it is usually the easiest approach. Other approaches like "Galerkin's" method could be applied, depending on how the problem lends itself to it.

Fig. 8 shows the results for such a calculation. The total number of modes (N modes) taken into consideration for

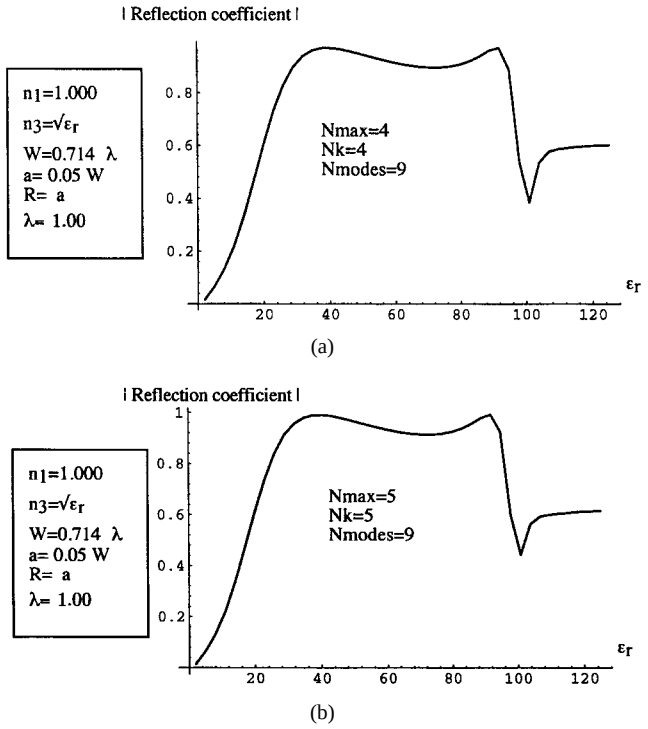

Fig. 8. Scattering by a dielectric disk inside a metallic waveguide. Point-matching approach.

expressing the scattered field determines the complexity of the system. As $Nmodes$ increases, the number of Fourier terms required to express the current $(Nmax)$ and the field (Nk) increases too. This is because the higher order evanescent modes decay faster, requiring more Fourier terms to express their rapid spatial decay. This increases the number of samples required to get a best fit for the current. One has to take a sufficiently large number of samples so that the results obtained from (36) and (37) converge within the desired numerical accuracy. For Fig. 8, this was approximately ten samples (uniform sampling) along the radial and angular directions, totalling approximately 100 uniformly distributed sample points within the disk. Even for a few terms, the results are remarkably good. The electric-field reflectivity increases and approaches 1.00 as the permittivity (ϵ_r) increases. The graph shows a resonant dip at around $\epsilon_r = 105$. The point where the resonant dip occurs varies, but converges as the number of modes $Nmodes$ increases, indicating that the scattered field is described with increasing accuracy and that the additional terms improve the accuracy only marginally.

2) Variational Approach: The current on the separatrix circle of radius R is sought, for use in an expression for the scattering coefficients. Symbolically, the currents are c; the Green's function is G and the given incident field inside the separatrix circle is f. Then, $G \cdot c = f$. However, we do not really need c (at least not to great accuracy); we really want the scattering coefficient $a = g \cdot c$, where g is a known operation on the current. In detail,

$$f(x,z) = \oint G(x,z;\theta) \cdot c(\theta)\, d\theta \tag{38}$$

$$a = \oint g(\theta) \cdot c(\theta)\, d\theta. \tag{39}$$

The integrations are around the periphery of the separatrix circle; $f(x,z)$ is known inside that circle.

As we cannot readily invert the Green's function operator, we seek a variational expression for a. We look for a solution to the adjoint problem, a field $b(x,z)$ such that the known $g(\theta)$ can be expressed in terms of the same Green's function by $g = b \cdot G$. If this adjoint field were at hand, we would have the following equivalent expressions for the scattering coefficient a:

$$a = g \cdot c = b \cdot G \cdot c = b \cdot f = \frac{b \cdot f\; g \cdot c}{b \cdot G \cdot c}.$$

The last of these is not only homogeneous in b and c, but variational too: if b and c change by δb and δc, then a changes by an amount proportional to $\delta b \delta c$. This means that a poor guess for b and c can yield fairly good estimates for a. In detail,

$$g(\theta) = \int b(x,z)\; \cdot G(x,z;\theta)\, dA \tag{40}$$

$$a = \int b(x,z) \cdot f(x,z)\, dA. \tag{41}$$

The integrations are over the interior of the separatrix circle. The variational expression for a is, in detail,

$$a = \frac{\int \oint b(x,z) \cdot f(x,z)\; g(\theta) \cdot c(\theta) d\theta\, dA}{\int \oint b(x,z) \cdot G(x,z;\theta) \cdot c(\theta)\, d\theta\, dA}. \tag{42}$$

From the modal expansions of fields and the LRT, we can express the Green's function, within the separatrix circle at least, as

$$G(x,z;\theta) = \sum_n W_n^+(x,z)\mu(z - z(\theta))W_n^-(x(\theta),z(\theta)) + \sum_n W_n^-(x,z)\mu(z(\theta) - z)W_n^+(x(\theta),z(\theta)) \tag{43}$$

where $\mu(\zeta)$ is the unit step function and the W's are normal modes of the waveguide. There are two values of a sought, one for the positive-traveling mode at $z > R$ and one for the negative-traveling mode at $z < -R$; each applies to a particular mode of the waveguide (subscript M is the incident mode). Again, from the LRT, we have

$$g_n^+(\theta) = W_n^-(x(\theta),z(\theta))$$
$$g_n^-(\theta) = W_n^+(x(\theta),z(\theta)).$$

Thus, we need to obtain reasonable estimates of both $b(x,z)$ and $c(\theta)$ so that even better estimates of a can be extracted from the variational expression.

Since the normal modes of the waveguide, which enter into the Green's function, are orthogonal over the entire plane, we can expect that, over just the separatrix's interior and especially if the circle is large, the adjoint field $b(x,z)$ should primarily be the incident mode, with significant contributions

from the other modes only if they are nearby in the spectrum. Retaining just $2K+1$ modes near the incident one, we have

$$b_M^+(x,z) = \sum_{k=-K}^{K} \beta_k^+ W_{M+k}^-(x,z) \tag{44}$$

$$b_M^-(x,z) = \sum_{k=-K}^{K} \beta_k^- W_{M+k}^+(x,z) \tag{45}$$

and we seek the best set of constants β. Similarly, the currents may be expressed as a Fourier series

$$c(\theta) = \sum_{l=-L}^{L} \gamma_l e^{jl\theta} \tag{46}$$

if we retain $2L+1$ harmonics. The unknowns are now the $2K+1$ constants β and the $2L+1$ constants γ. The required integrations can be done once and for all (not necessarily in closed form) as

$$D_{k,l} = \int \oint W_{M+k}(x,z) \cdot G(x,z;\theta)\, e^{jl\theta}\, d\theta\, dA \tag{47}$$

$$N_{k,l} = \int W_{M+k}(x,z) \cdot f(x,z)\, dA \cdot \oint W_{M+l}(x(\theta),z(\theta)) \cdot \hat{\gamma}_l\, e^{jl\theta} \tag{48}$$

and $\hat{\gamma}_l$ is unit vector along the current. We have two of each of these—one for each direction of propagation.

The variational expression for the constant vectors β and γ is just

$$a = \frac{\beta \cdot N \cdot \gamma}{\beta \cdot D \cdot \gamma}. \tag{49}$$

On differentiating with respect to each of these vectors, it follows that the optimal solution is given by

$$\beta \cdot [N - aD] = 0 \tag{50}$$

and

$$[N - aD] \cdot \gamma = 0 \tag{51}$$

i.e., β and γ are annihilated by the matrix $N - aD$. Note that this matrix has $2K+1$ rows and $2L+1$ columns. If $K = L$, then the matrix is square and the variational solution for a is a root of the characteristic equation

$$\det[N - aD] = 0. \tag{52}$$

If $K \neq L$, then the corresponding condition requires the rank of the nonsquare matrix to be sufficiently low. The condition is effectively written as

$$\det \begin{bmatrix} N - aD & 0 \\ 0 & (N - aD)^T \end{bmatrix} = 0. \tag{53}$$

The eigenvalue with the largest absolute value is the one that is selected. The results for such a calculation are shown in Fig. 9. They are in accordance with earlier results [18], [19] in the form of the curve, except for the point where the resonance dip occurs. Our results show the resonant dip to occur at slightly lower (5% lower at 105) permittivity than shown in previous results. However, we believe our results to be more accurate. First, there are no approximations made as far as modeling of the scattered field is concerned and, more important, our results from point matching and the variational method are consistent.

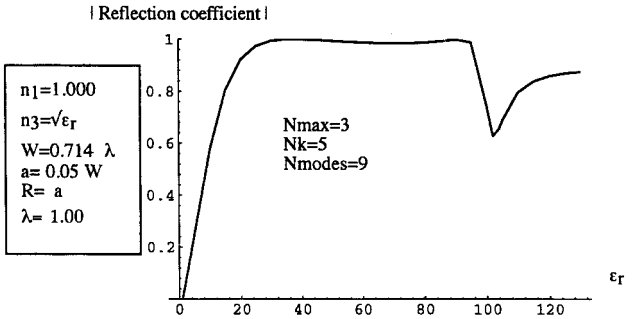

Fig. 9. Scattering by a dielectric disk inside a metallic waveguide. Variational approach.

VI. Concluding Remarks

The problem of coupling between a dielectric ring/disk and a dielectric slab waveguide has been solved analytically by reducing the problem to two simultaneous (but simpler and solvable) independent problems involving the ring and waveguide alone. The method is fairly general and can be applied to other geometries and problems. The method is most efficient for small radii of curvatures (relative to wavelength) and yields fast-converging solutions. For large radii, the numerical complexity increases. Since the two problems are independent, we can apply various levels of approximations to find the currents e_l, m_l. The original intractable problem requiring boundary conditions across two different geometries is now reduced to the simpler problem of finding the currents. The solution can be made progressively more accurate by taking a larger number of terms into consideration.

The usefulness of the method of equivalence is not in obtaining another numerical method, but in making simplifying approximations and coming up with accurate analytic solutions [20]. This will be stressed in subsequent papers.

Appendix

On applying the continuity conditions at the interface $r = r_1$, we get in matrix form

$$E_l \cdot \begin{bmatrix} J_l(k_0 n_3 r_1) \\ J_l'(k_0 n_3 r_1) \end{bmatrix} = \begin{bmatrix} J_l(k_0 n_g r_1) & Y_l(k_0 n_g r_1) \\ (n_g/n_3)\, J_l'(k_0 n_g r_1) & (n_g/n_3)\, Y_l'(k_0 n_g r_1) \end{bmatrix} \cdot \begin{bmatrix} C_l \\ D_l \end{bmatrix}. \tag{54}$$

Similarly, at $r = r_2$,

$$\begin{bmatrix} J_l(k_0 n_g r_2) & Y_l(k_0 n_g r_2) \\ (n_g/n_3)\, J_l'(k_0 n_g r_2) & (n_g/n_3)\, Y_l'(k_0 n_g r_2) \end{bmatrix} \cdot \begin{bmatrix} C_l \\ D_l \end{bmatrix} = \begin{bmatrix} J_l(k_0 n_1 r_2) & Y_l(k_0 n_1 r_2) \\ (n_1/n_3)\, J_l'(k_0 n_1 r_2) & (n_1/n_3)\, Y_l'(k_0 n_1 r_2) \end{bmatrix} \cdot \begin{bmatrix} A_l \\ B_l \end{bmatrix}. \tag{55}$$

The field needs to satisfy boundary discontinuity conditions at the current source at $r = R$, given by [13, Ch. 2, pp. 19–20]

$$\hat{r} \times (\mathcal{H}_\theta^{\text{in}}(r,\theta) - \mathcal{H}_\theta^{\text{out}}(r,\theta)) = -\mathcal{J}_e$$
$$\hat{r} \times (\mathcal{E}_y^{\text{in}}(r,\theta) - \mathcal{E}_y^{\text{out}}(r,\theta)) = \mathcal{J}_m.$$

The superscripts *in* and *out* signify the regions inside $(r < R)$ and outside $(r > R)$ the current-carrying circle, respectively. Substituting

$$\mathcal{E}_y^{\text{out}}(r,\theta) = 0$$
$$\mathcal{H}_\theta^{\text{out}}(r,\theta) = 0$$
$$\mathcal{H}_\theta^{\text{in}}(r,\theta) = \frac{-j}{\omega\mu_0} \frac{\partial}{\partial r} \mathcal{E}_y^{\text{in}}(r,\theta)$$

and expanding the field and current in terms of Fourier series and equating term-by-term results in

$$\mathcal{J}_e = \sum_l \frac{jk_0 n_1}{\omega\mu_0} \left(A_l J_l'(k_0 n_1 R) + B_l Y_l'(k_0 n_1 R)\right) e^{jl\theta}\, \hat{y} \tag{56}$$

$$\mathcal{J}_m = -\sum_l \left(A_l J_l(k_0 n_1 R) + B_l Y_l(k_0 n_1 R)\right) e^{jl\theta}\, \hat{\theta} \tag{57}$$

where $'$ signifies the derivative with respect to the argument. The factor (B_l/A_l) is determined from the boundary conditions at $r = r_1$ and $r = r_2$.

A. The Ratio (B_l/A_l)

The boundary conditions for interfaces r_1, r_2 can be rewritten as

$$E_l \cdot \begin{bmatrix} J_l(k_0 n_3 r_1) \\ J_l'(k_0 n_3 r_1) \end{bmatrix} = M_g(r_1) \cdot \begin{bmatrix} C_l \\ D_l \end{bmatrix} \tag{58}$$

$$M_g(r_2) \cdot \begin{bmatrix} C_l \\ D_l \end{bmatrix} = M_1(r_2) \cdot \begin{bmatrix} A_l \\ B_l \end{bmatrix}. \tag{59}$$

These combine into

$$M_1^{-1}(r_2) \cdot M_g(r_2) \cdot M_g^{-1}(r_1) \cdot \begin{bmatrix} J_l(k_0 n_3 r_1) \\ J_l'(k_0 n_3 r_1) \end{bmatrix} = \begin{bmatrix} A_l/E_l \\ B_l/E_l \end{bmatrix} \tag{60}$$

where

$$M_1^{-1}(r_2) = \begin{bmatrix} J_l(k_0 n_1 r_2) & Y_l(k_0 n_1 r_2) \\ (n_1/n_3)\, J_l'(k_0 n_1 r_2) & (n_1/n_3)\, Y_l'(k_0 n_1 r_2) \end{bmatrix}^{-1}$$
$$= (\pi k_0 n_3 r_2/2) \begin{bmatrix} (n_1/n_3)\, Y_l'(k_0 n_1 r_2) & -Y_l(k_0 n_1 r_2) \\ -(n_1/n_3)\, J_l'(k_0 n_1 r_2) & J_l(k_0 n_1 r_2) \end{bmatrix}$$

and, similarly, for the other matrices and inverses.

Use has been made of the fact that the Wronskian of $\{J_l(x), Y_l(x)\}$ equals $2/(\pi x)$. Equation (60) can be solved for the ratio $B_l/A_l = \Delta_l$ simply by matrix multiplication. It can be written explicitly as

$$\Delta_l = \frac{[0\ 1] \cdot M_{\text{eq}} \cdot J}{[1\ 0] \cdot M_{\text{eq}} \cdot J} \tag{61}$$

where J is the transpose of $[J_l(k_0 n_3 r_1)\ J_l'(k_0 n_3 r_1)]$ and

$$M_{\text{eq}} = M_1^{-1}(r_2) \cdot M_g(r_2) \cdot M_g^{-1}(r_1).$$

In the special case when the dielectric ring degenerates into a disk, i.e.,

$$r_2 \to r_1 = a$$

(60) reduces to

$$M_1^{-1}(a) \cdot \begin{bmatrix} J_l(k_0 n_3 a) \\ J_l'(k_0 n_3 a) \end{bmatrix} = \begin{bmatrix} A_l/E_l \\ B_l/E_l \end{bmatrix}. \tag{62}$$

On expanding and simplifying, the expression yields

$$\Delta_l = \frac{n_3 J_l(k_0 n_1 a) J_l'(k_0 n_3 a) - n_1 J_l'(k_0 n_1 a) J_l(k_0 n_3 a)}{n_1 J_l(k_0 n_3 a) Y_l'(k_0 n_1 a) - n_3 J_l'(k_0 n_3 a) Y_l(k_0 n_1 a)}. \tag{63}$$

REFERENCES

[1] H. Han, M. E. Favaro, D. V. Forbes, J. J. Coleman, "$In_xGa_{1-x}As$-$Al_yGa_{1-y}As$-GaAs strained-layer quantum-well heterostructure circular ring lasers," *IEEE Photon. Technol. Lett.*, vol. 4, pp.817–819, Aug. 1992.

[2] A. S.-H. Liao and S. Wang, "Semiconductor injection lasers with a circular resonator," *Appl. Phys. Lett.*, vol. 36, no. 10, pp. 801–803, May 1980.

[3] A. F. Jezierski and P. J. R. Laybourn, "Integrated semiconductor ring lasers," *Proc. Inst. Elect. Eng.*, vol. 135, pt. J. no. 1, pp. 17–24, Feb. 1988.

[4] J. P. Hohimer, G. A. Vawter, D. C. Craft, G. R. Hadley, and M. E. Warren, "Single-frequency continuous-wave operation of a ring resonator diode laser," *Appl. Phys. Lett.*, vol. 59, pp. 3360–3362, 1991.

[5] J. P. Hohimer, G. A. Vawter, D. C. Craft, and G. R. Hadley, "Interferometric ring diode lasers," *Appl. Phys. Lett.*, vol. 61, pp. 1375–1377, 1992.

[6] J. P. Hohimer, G. A. Vawter, D. C. Craft, and G. R. Hadley, "Improving the performance of semiconductor ring lasers by controlled reflection feedback," *Appl. Phys. Lett.*, vol. 61, pp. 1013–1015, 1992.

[7] J. P. Hohimer, G. A. Vawter, and D. C. Craft, "Unidirectional operation in a semiconductor ring diode laser," *Appl. Phys. Lett.*, vol. 62, pp. 1185–1187, 1993.

[8] S. Wang, H. K. Choi, and I. H. Fatttah, "Studies of semiconductor lasers of the interferometric and the ring types," *IEEE J. Quantum Electron.*, vol. QE-18, pp. 610–617, Apr. 1982.

[9] R. F. Nabiev, D. Francis, and C. J. Chang-Hasnain, "Lateral and longitudinal mode discrimination in index-guided circular ring semiconductor lasers," *IEEE Photon. Technol. Lett.*, vol. 5, pp. 975–978, Sept. 1993.

[10] R. S. Burton, T. E. Schlesinger, and M. Munowitz, "An investigation of the modal coupling of simple branching semiconductor ring lasers," *J. Lightwave Technol.*, vol. 12, pp. 755–759, May 1994.

[11] M. Heiblum and J. Harris, "Analysis of curved optical waveguides by conformal transformation," *IEEE J. Quantum Electron.*, vol. QE-11, pp. 75–83, Feb. 1975.

[12] E. Yamashita, *Analysis Methods for Electromagnetic Wave Problems*. Norwood, MA: Artech House, 1990.

[13] R. E. Collin, *Field Theory of Guided Waves*, 2nd ed. New York: IEEE Press, 1991.

[14] D. Marcuse, *Light Transmission Optics*, 2nd ed. New York: Van Nostrand, 1982.

[15] M. Abramowitz and I. A. Stegun, *Handbook of Mathematical Functions with Formulas, Graphs and Mathematical Tables*. New York: Wiley, 1972.

[16] D. Marcuse, *Theory of Dielectric Optical Waveguides*, 2nd ed. New York: Academic, 1992.

[17] N. Bleistein and R. A. Handelsman, *Asymptotic Expansions of Integrals*. New York: Holt, Rinehart and Winston, 1974.

[18] D. E. Nielsen, "Scattering by a cylindrical post of complex permittivity in a waveguide," *IEEE Trans. Microwave Theory Tech.*, vol. MTT-17, pp. 148–153, Mar. 1969.

[19] J. C. Araneta, "High temperature microwave characterization of dielectric rods," *IEEE Trans. Microwave Theory Tech.*, vol. MTT-32, pp. 1328–35, Oct. 1984.

[20] R. Dehmubed, "Coupling between slab waveguide and a dielectric ring," Ph.D. dissertation, Dept. Elect. Eng., Columbia Univ., New York, NY, 1997.

Rohinton S. Dehmubed (M'87) received the B.Tech. degree in electrical engineering from the Indian Institute of Technology, Bombay, India, in 1987, and the Ph.D. degree from Columbia University, New York, NY, in 1997.

He has worked in the field of optical devices, optical network design, and free-space optics. Since June 1997, he has been working in the field of high-speed telecommunications IC design at TranSwitch Corporation, Shelton, CT.

Paul Diament was born in Paris, France. He received the B.S., M.S., and Ph.D. degrees in electrical engineering from Columbia University, New York, NY, in 1960, 1961, and 1963, respectively.

In 1963, he joined the faculty of Columbia University, and is currently a Professor of electrical engineering, specializing in electromagnetics. His teaching and research areas are in all phases of electromagnetics and wave propagation, including microwaves, antennas, lightwave systems, optics, radiation statistics, plasmas, wave interactions, relativistic electron beams, and transient electromagnetic phenomena. He has also delved into stochastic processes, which are applied to fluctuations in financial markets. He authored *Wave Transmission and Fiber Optics* (New York: Macmillian, 1990), and is currently authoring the undergraduate textbook in electromagnetics *Concepts in Electromagnetics* (Englewood Cliffs, NJ: Prentice-Hall).